Frontiers in Bioscience Landmark

Front. Biosci. (Landmark Ed) **2026**; 31(8): 49685
https://doi.org/10.31083/FBL49685

Original Research

PCSK9 as a Key Gene of Metastasis in Lung Adenocarcinoma: A Multi-omics and Experimental Validation Study

Dan Zong[1], Dejun Wang[1], Luxi Qian[1], Ning Jiang[1], Lijun Zhao[1], Cheng Chen[1], Xia He[1,*]

[1]Department of Radiation Oncology, Jiangsu Cancer Hospital, 210009 Nanjing, Jiangsu, China
*Correspondence: hexiabm163@163.com (Xia He)
Academic Editor: Peter Brenneisen
Submitted: 4 January 2026 Revised: 26 April 2026 Accepted: 15 May 2026 Published: 14 August 2026

Abstract

Background: Lung adenocarcinoma (LUAD) is the most common form of lung cancer. Proprotein convertase subtilisin/kexin type 9 (PCSK9) is abnormally expressed in various tumor tissues and is associated with malignant phenotypes. However, the clinical significance, function, and mechanism of LUAD invasion and metastasis remain unclear. **Methods:** We retrospectively enrolled 100 patients with LUAD in this study. Initially, qRT-PCR was performed to detect PCSK9 levels in clinical tissues. Subsequently, bioinformatics analysis of scRNA-seq and The Cancer Genome Atlas Program (TCGA) datasets was performed to predict the role of PCSK9 in tumor cell malignancy and its potential downstream pathways. These predictions were validated experimentally using the CCK-8 assay, TUNEL staining, wound healing, transwell invasion assay, and an *in vivo* lung metastasis model. Finally, Western blotting and an AKT inhibitor (MK2206) were used to verify the underlying mechanism. **Results:** PCSK9 was significantly upregulated in LUAD tissues compared to paracancerous tissues and was associated with poorer OS and DFS. Bioinformatics analysis of scRNA-seq data and TCGA analysis predicted that PCSK9 is highly enriched in tumor cells and is involved in EMT, and that the PI3K/AKT pathway plays a significant role in LUAD development. Experiments confirmed that PCSK9 markedly promoted LUAD cell proliferation, migration, and invasion *in vitro* and lung metastasis *in vivo*. PCSK9 overexpression significantly upregulated p-AKT, p-PI3K, and p-mTOR levels. Furthermore, the AKT inhibitor, MK2206, reversed the promoting effects of PCSK9. **Conclusions:** PCSK9 expression is associated with the prognosis and diagnosis of LUAD. This molecule activates the PI3K/AKT signaling pathway, thereby driving invasion, metastasis, and proliferation in LUAD.

Keywords: proprotein convertase subtilisin/kexin type 9; adenocarcinoma of lung; phosphatidylinositol 3-kinases; proto-oncogene proteins c-akt; prognosis

1. Introduction

Lung cancer, a common malignant tumor, has a persistently high incidence and mortality rate and has drawn significant attention from the medical community [1,2]. The International Agency for Research on Cancer (IARC) has further substantiated this perspective, estimating approximately 2.02 million new lung cancer cases and approximately 1.76 million related deaths [3]. Lung adenocarcinoma (LUAD) is distinguished by its significant malignancy and is one of the most prevalent subtypes of lung cancer. Invasion and metastasis associated with LUAD can accelerate disease progression and serve as primary contributors to the poor prognosis observed in patients [4]. Furthermore, owing to a lack of effective targeted sites, current targeted therapies face considerable challenges in achieving precise control [5,6].

Proprotein convertase subtilisin/kexin type 9 (PCSK9) is a serine protease that plays a crucial role in reducing the clearance efficiency of low-density lipoprotein (LDL). It achieves this by degrading low-density lipoprotein receptors (LDLR) located on the surface of hepatocytes, which leads to an elevation in plasma cholesterol levels [7,8,9]. However, LUAD cells often undergo metabolic reprogramming and abnormal cholesterol metabolism is one of the most common characteristics. In addition, numerous studies have demonstrated that PCSK9 is remarkably expressed in malignant tumor tissues and is intricately linked to the advancement of tumors, indicating that PCSK9 may participate in tumor progression [10,11]. Wang et al. [10] showed that PCSK9 drives colon cancer progression and metastasis via EMT and phosphoinositide 3-kinase/protein kinase B (PI3K/AKT) signaling in tumor cells as well as macrophage polarization. Bonaventura et al. [12] demonstrated that PCSK9 is a promising prognostic marker in lung cancer. Therefore, we inferred that PCSK9 might promote tumor progression in LUAD. Nonetheless, the clinical significance, function, and underlying mechanisms of PCSK9 in the invasion and metastasis of LUAD remain unclear.

Therefore, this study suggests that PCSK9 may mediate the metastasis of LUAD cells via the PI3K/AKT signaling cascade. This discovery provides a theoretical foundation for optimizing the treatment strategies for LUAD.

2. Materials and Methods

2.1 Processing of Publicly Available Transcriptome Data

The Cancer Genome Atlas Program (TCGA) provides RNA sequencing data, clinical information, and gene expression profiles of LUAD. The Kaplan-Meier method was used to plot survival curves based on different PCSK9 expression levels using the *survminer* R package. The Log-rank test was used to analyze the differences in survival outcomes. Genes differentially expressed between the PCSK9-high and PCSK9-low groups were identified ($|\log_2 FC| > 1$, $p < 0.05$), visualized with a volcano plot, and analyzed for GO and KEGG enrichment using DAVID 6.8 (version 6.8, Bethesda, MD, USA).

2.2 Tissue Samples

This study complied with the Declaration of Helsinki and was approved by the Ethics Committee (Ethic Approval Number: 2021-017). Written informed consent was obtained from 100 patients prior to the study for the use of biological samples in the experiments and data analysis. Cancerous tissues and corresponding para-cancerous tissues (at least 3–4 cm away from the margin of the cancerous tissue, confirmed to be free of tumor cell infiltration by pathological examination) from 100 patients with LUAD were retrospectively incorporated into this study. Inclusion criteria: Patients were eligible for enrollment if they met all of the following criteria: Histologically confirmed non-small cell lung cancer (NSCLC) with adenocarcinoma subtype, according to the 2021 World Health Organization (WHO) Classification of Thoracic Tumors; Stage I–IV NSCLC, staged according to the 8th Edition of the American Joint Committee on Cancer (AJCC) Tumor-Node-Metastasis (TNM) Staging System; Age: 18–80 years at the time of informed consent; Performance status: Eastern Cooperative Oncology Group (ECOG) performance status of 0 or 1. Exclusion criteria: Patients with concurrent or prior active malignancies; Patients with severe or ncontrolled comorbities; Patients with poor performance status; Patients who refused to provide informed consent. All patients were 35–78 years old (median age: 62 years), with pathological stages ranging from I to IV, comprising Stage I (28 cases), Stage II (35 cases), Stage III (22 cases), and Stage IV (15 cases). All diagnoses were confirmed by a senior pathologist with more than five years of work experience. After collection, all the samples were immediately cryopreserved in liquid nitrogen for subsequent experiments.

2.3 Quantitative Reverse Transcription Polymerase Chain Reaction (qRT-PCR)

Total RNA was extracted from tissues or cells using TRIzol reagent (Invitrogen, Carlsbad, CA, USA) and reverse-transcribed using the PrimeScript RT Master Mix Kit (RR036A, TaKaRa, Dalian, China). PCSK9 mRNA expression was detected using SYBR Green fluorescence and calculated using the $2^{-\Delta\Delta CT}$ method, with GAPDH as an internal control. PCR conditions were 95 °C for 5 s, 63 °C for 30 s, and 72 °C for 30 s for 35 cycles. PCSK9: F 5′-ATACAGAGTGACCACCGGA-3′, R 5′-TCACACTTGCTGGCCTGTC-3′; internal reference GAPDH: F 5′-GCACCGTCAAGGCTGAGAAC-3′, R 5′-TGGTGAAGACGCCAGTGGA-3′.

2.4 Cell Culture

BEAS-2B (CRL-3588), and NCI-H1975 (CRL-5908) cells (ATCC, Manassas, VA, USA) were cultured in RPMI-1640 medium (Gibco, Grand Island, NY, USA) supplemented with 10% FBS (Thermo Fisher Scientific, Waltham, MA, USA), 100 U/mL penicillin, and 100 µg/mL streptomycin (Sigma-Aldrich, St. Louis, MO, USA) under 5% CO_2. Mycoplasma testing was conducted every three months using a detection kit (LT07, Lonza, Basel, Switzerland). All cell lines were validated by STR profiling and tested negative for Mycoplasma.

2.5 Plasmid Construction and Stably Transfected Cell Lines

The nucleotide sequence of PCSK9 was retrieved from the NCBI database and primers for the PCSK9 gene (upstream primer: 5′-CGGAATTCATGGCGGCCGCCACCATG-3′, downstream primer: 5′-CCCAAGCTTTCAGCTGGCCGTCCTCGTC-3′) were used. The coding sequence of PCSK9 was amplified by PCR and subsequently introduced into the pLenti-CMV-Puro vector (Addgene, Watertown, MA, USA). The lentiviral vector (oe-PCSK9) and control vector (oe-NC) were constructed, and the inserted sequence was verified by sequencing. pLenti-PCSK9 and PMD2.G (Addgene) were cotransfected into 293T cells. The supernatants were collected, centrifuged at 1000 rpm for 5 min to remove impurities, and used to infect PC-9 (BNCC340767) (BNCC, Beijing, China) and NCI-H1975 cells. After infection, 2 µg/mL puromycin (InvivoGen, San Diego, CA, USA) was administered for stable cell line screening, followed by the isolation of monoclonal cells with comparable levels of PCSK9 transcripts by limiting dilution for subsequent analysis.

2.6 Western Blotting Analysis

Total protein was extracted from the cells, separated by SDS-PAGE (Bio-Rad, Hercules, CA, USA), and transferred onto PVDF membranes (Millipore, Billerica, MA, USA). The membranes were blocked with 5% skim milk for 2 h at room temperature, then incubated overnight at 4 °C with primary antibodies against PCSK9 (Rabbit, 85813, 1:1000), p-AKT (Rabbit, 9271, 1:2000), and β-actin (Rabbit, 4967, 1:3000) (all from Cell Signaling Technology, Danvers, MA, USA). After washing with TBST, membranes were incubated with horseradish peroxidase-conjugated secondary antibodies (Goat anti-rabbit, 7074,

Table 1. Analysis of the correlation between PCSK9 and clinical features.

Clinical Data	Expression of PCSK9 mRNA		χ^2	*p* value
	Low, N = 50	High, N = 50		
Age				
>60	31	27	0.657	0.418
≤60	19	23		
Gender				
Male	40	39	0.060	0.806
Female	10	11		
TNM Stage				
I&II	43	20	22.690	<0.001***
III&IV	7	30		
KPS				
≥90	38	36		
<90 and ≥80	6	9	0.745	0.689
<80 and ≥70	6	5		

TNM, Tumor Node Metastasis; KPS, Karnofsky Performance Status.
***$p < 0.001$.

1:2000) (all from Cell Signaling Technology, Danvers, MA, USA). Protein bands were visualized using enhanced chemiluminescence, quantified with ImageJ software (version 1.8.0, Bethesda, MD, USA), and target protein expression was normalized to β-actin.

2.7 Cell Counting Kit-8 (CCK-8) Assay

The cells were adjusted to 1×10^4 cells/mL and seeded into 96-well plates (1×10^3 cells/well). At 0, 24, 48, and 72 h post-seeding, 10 µL of the CCK-8 reagent was added to each well. After gentle shaking, the absorbance was measured at 450 nm using a microplate reader (Molecular Devices, San Jose, CA, USA) to assess cell proliferation.

2.8 Terminal Deoxynucleotidyl Transferase dUTP Nick End Labeling (TUNEL) Staining

PC-9 and NCI-H1975 cells were pre-treated with PBS, and 0.1% Triton X-100 (Sigma-Aldrich) was added. The reaction mixture containing the TdT enzyme was used in the TUNEL assay kit (Roche, Basel, Switzerland), alongside a parallel negative control that omitted the TdT enzyme. After incubation, the cells were counterstained with 1 µg/mL DAPI (Invitrogen). After three washes with PBS to remove unbound DAPI, coverslips were mounted and the fields were examined under a fluorescence microscope (Olympus, Tokyo, Japan). Note: All procedures following addition of the reaction mixture must be conducted in the dark. The apoptotic rate (%) was calculated as follows: (Number of TUNEL–positive cells/total cell number) × 100.

2.9 Single-cell RNA Sequencing (scRNA-seq) Dataset

The GSE149655 (including two patients with primary LUAD) and GSE143423 (including three LUAD patients with brain metastasis) datasets were obtained from the GEO database (https://www.ncbi.nlm.nih.gov/geo/). GSE149655 and GSE143423 were then processed using the Seurat R package to generate Seurat objects. The cell filtration criteria were referenced from other studies [13,14], and 13,595 cells were finally obtained. The top 2000 highly variable genes were identified using "FindVariableFeatures" and "NormalizeData", followed by PCA across all samples. The first 50 principal components were used for the downstream analysis. The clusters were visualized using the UMAP dimensionality reduction technique. Next, the cells were annotated. Automatic annotation: Cell population marker genes in the Seurat object were annotated using the "Hspe. Human annotation" file from the "SingleR" SingleR package. Manual annotation: CopyKAT distinguished between tumor and epithelial cells, with subsequent tumor subset extraction via Seurat's subset function. CDS objects were generated from Seurat expression matrices with cell metadata and gene annotations using Monocle3 preprocessing functions. UMAP dimensionality reduction and trajectory analysis were conducted using clustering and graph-learning algorithms, with primary tumor cells designated as trajectory roots. Pseudotime-associated genes were subsequently identified and visualized using trajectory-plot modules. GO and KEGG enrichment analyses were performed as previously described [15].

2.10 Scratch Healing Assay

Cells were seeded in 6-well plates at 80–90% confluence, starved in serum-free medium for 24 h, scratched with a 10 µL pipette tip, and washed three times with PBS. After incubation in serum-free medium at room temperature, phase-contrast images were captured at 0 and 24 h. Wound healing rate was calculated using ImageJ as $(\text{width}_{0\,h} - \text{width}_{24\,h}) / \text{width}_{0\,h} \times 100\%$.

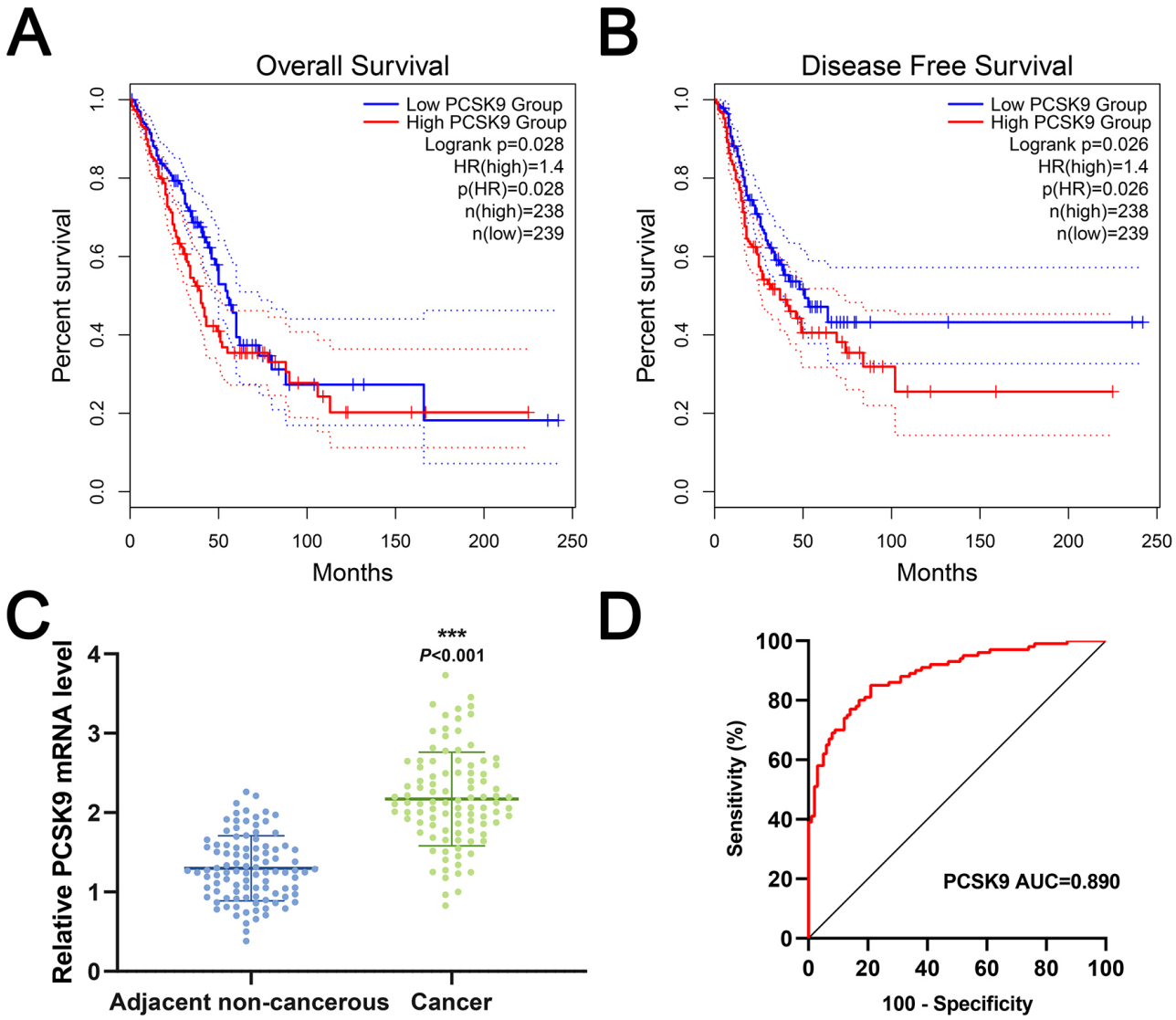

Fig. 1. PCSK9 is related to the prognosis and diagnosis of LUAD. (A) Comparison of OS between the two groups (high PCSK9 expression vs. low PCSK9 expression). (B) Comparison of two groups of DFS. (C) The mRNA expression level of PCSK9 in 100 cases was detected by qRT-PCR. ***$p < 0.001$. (D) ROC curve analysis of PCSK9 for the diagnosis of LUAD. PCSK9, proprotein convertase subtilisin/kexin type 9; LUAD, lung adenocarcinoma; OS, overall survival; DFS, disease-free survival; qRT-PCR, quantitative reverse transcription polymerase chain reaction; ROC, receiver operating characteristic.

2.11 Transwell Assay

The Transwell assay was performed using Matrigel (1:8 dilution, 50 µL/chamber, solidified for 4–6 h). Cells (5×10^4/100 µL) were seeded in the upper chamber and 10% FBS-containing medium was placed in the lower chamber. After incubation, adherent cells on the lower membrane were fixed with 4% methanol (Sigma-Aldrich), stained with crystal violet, and counted using the ImageJ software.

2.12 Establishment of Mouse Lung Metastasis Model

SPF BALB/c male nude mice (4- to 6-week-old, 15–20g, Charles River Laboratories, Wilmington, MA, USA) were randomly divided into four groups (n = 6 for each group): control, oe-NC, oe-PCSK9, and oe-PCSK9 + MK2206. The feeding environment was strictly regulated to maintain 24 °C, accompanied by a 12 h light-dark cycle. The PC-9 cells in each group were harvested and adjusted to a concentration of 1×10^7 cells/mL. No animals were excluded from the analysis. Subsequently, an aliquot of 0.1 mL of this cell suspension was administered via tail vein injection to each nude mouse. The PCSK9 + MK2206 group was treated with 10 µM MK2206 (Selleck Chemicals, Houston, TX, USA) 2 h before injection. Mice were observed over a 4-week period. After the recording ended, mice were anesthetized with isoflurane (3% for induction and 1.5% for maintenance) and then exposed to 80% CO_2 in a chamber for at least 5 min, followed by cervical disloca-

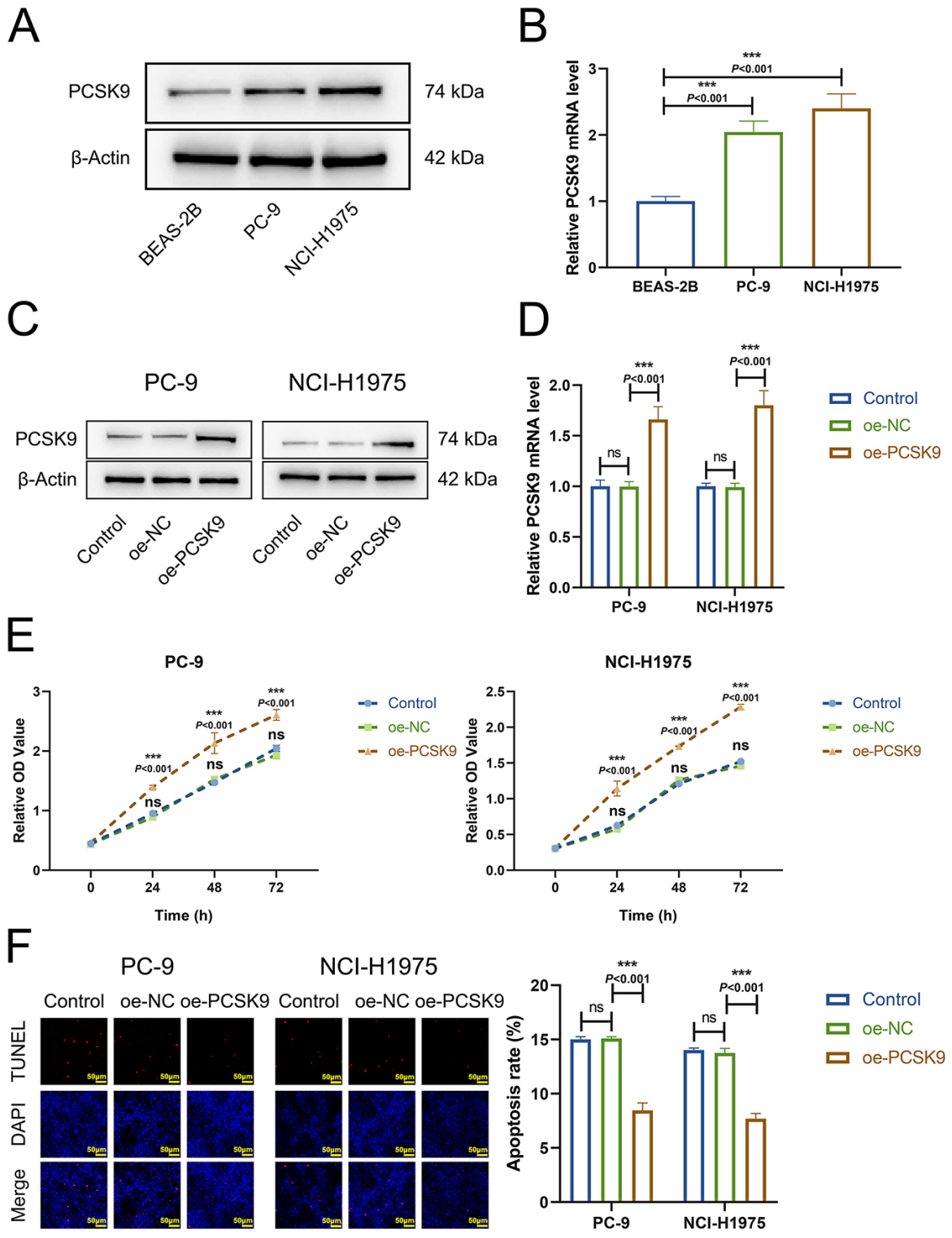

Fig. 2. PCSK9 promotes the proliferation of LUAD cells. (A,B) The protein and mRNA expression of PCSK9 in BEAS-2B cells and LUAD cell lines was detected by Western blotting and qRT-PCR. (C,D) Western blotting and qRT-PCR were used to verify the overexpression efficiency of PCSK9 in LUAD cell lines. (E) The CCK-8 assay was performed to detect cell viability. (F) TUNEL staining was used to verify the apoptotic activity of cells (Scale bar: 50 μm). Data are presented as the mean ± SD. n = 3 (technical replicates). One-way ANOVA was conducted. ns represents no significant, ***$p < 0.001$. CCK-8, Cell Counting Kit-8; TUNEL, terminal deoxynucleotidyl transferase dUTP nick end labeling.

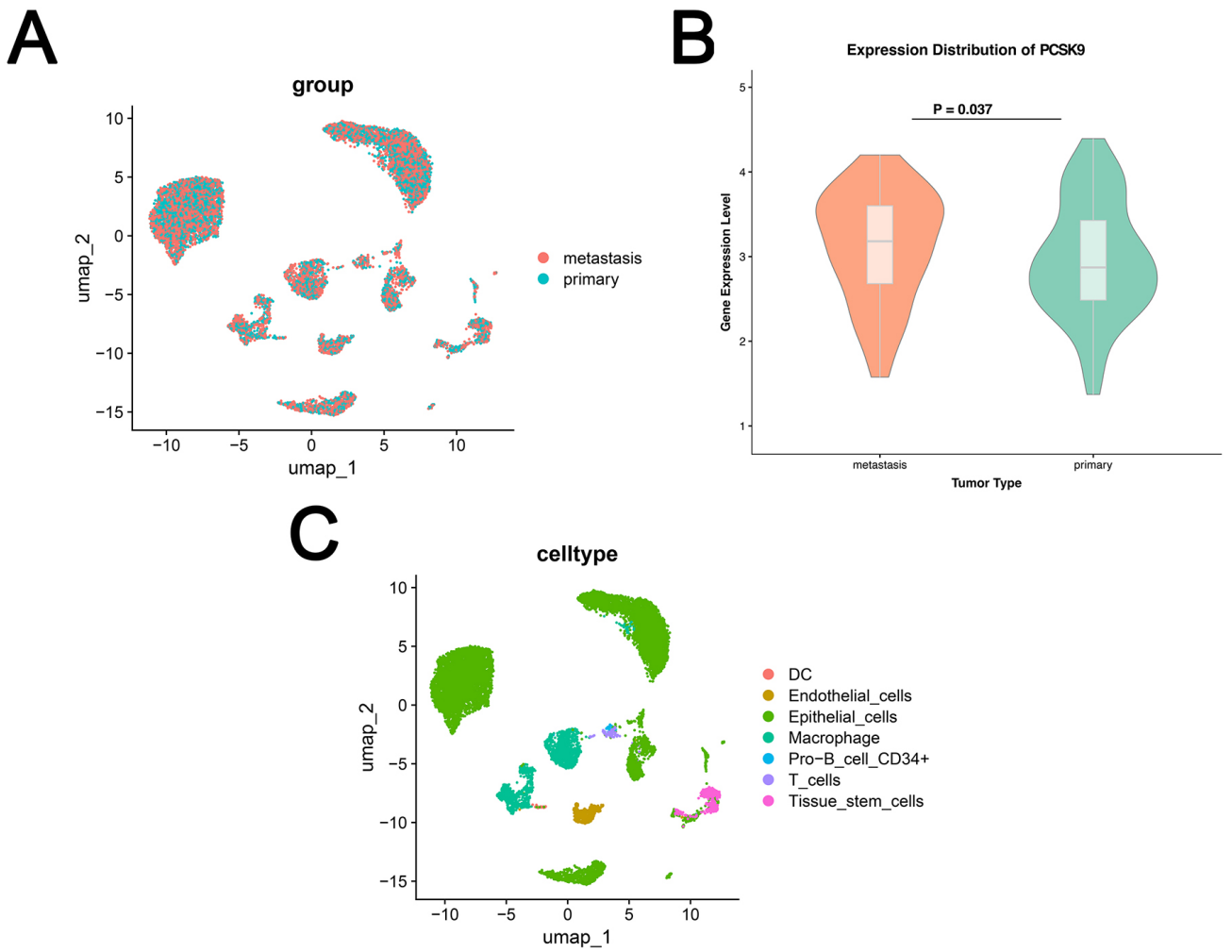

Fig. 3. PCSK9 is strongly associated with metastasis in LUAD. (A) The integrated UMAP of metastasis and primary LUAD patients. (B) Comparison of PCSK9 expression in metastasis and primary LUAD patients. (C) UMAP plot showing 7 cell types in metastasis and primary LUAD patients. UMAP, uniform manifold approximation and projection.

tion. The lungs were harvested, rinsed with PBS, and photographed. Metastatic nodules on the surface were counted.

2.13 Statistical Analysis

All statistical analyses were performed using SPSS version 25.0 (IBM, Chicago, IL, USA). The chi-square test was applied to count data, while measurement data were expressed as mean ± SD. The Shapiro-Wilk test assesses the normal distribution. Paired and independent *t*-tests were used for within-group and two-group comparisons, respectively, and one-way ANOVA with Tukey's post-hoc test was used for multiple groups. ROC curve analysis was performed to evaluate the diagnostic value of PCSK9 for LUAD by calculating the area under the curve (AUC), sensitivity, and specificity. Statistical significance was set at $p < 0.05$.

3. Results

3.1 PCSK9 is Related to Prognosis and Diagnosis of LUAD

We initially evaluated its prognostic value in LUAD using the TCGA dataset. Kaplan–Meier analysis showed that high PCSK9 expression was associated with significantly worse OS and DFS compared to low expression ($p = 0.028$, Fig. 1A; $p = 0.026$, Fig. 1B). PCSK9 levels were significantly higher in LUAD tissues than in the adjacent normal tissues (n = 100) ($p < 0.001$, Fig. 1C). No marked correlation was found between the magnitude of PCSK9 expression and patients' clinical attributes, such as age ($p = 0.418$), gender ($p = 0.806$), and KPS score ($p = 0.689$) (Table 1). Nonetheless, increased PCSK9 expression correlated with increased TNM staging ($p < 0.001$, Table 1). Finally, the AUC value of PCSK9 for the diagnosis of LUAD using ROC curve analysis was 0.890 (Fig. 1D). These findings indicate that PCSK9 correlates with worse outcomes in LUAD and is significantly elevated in LUAD tissue.

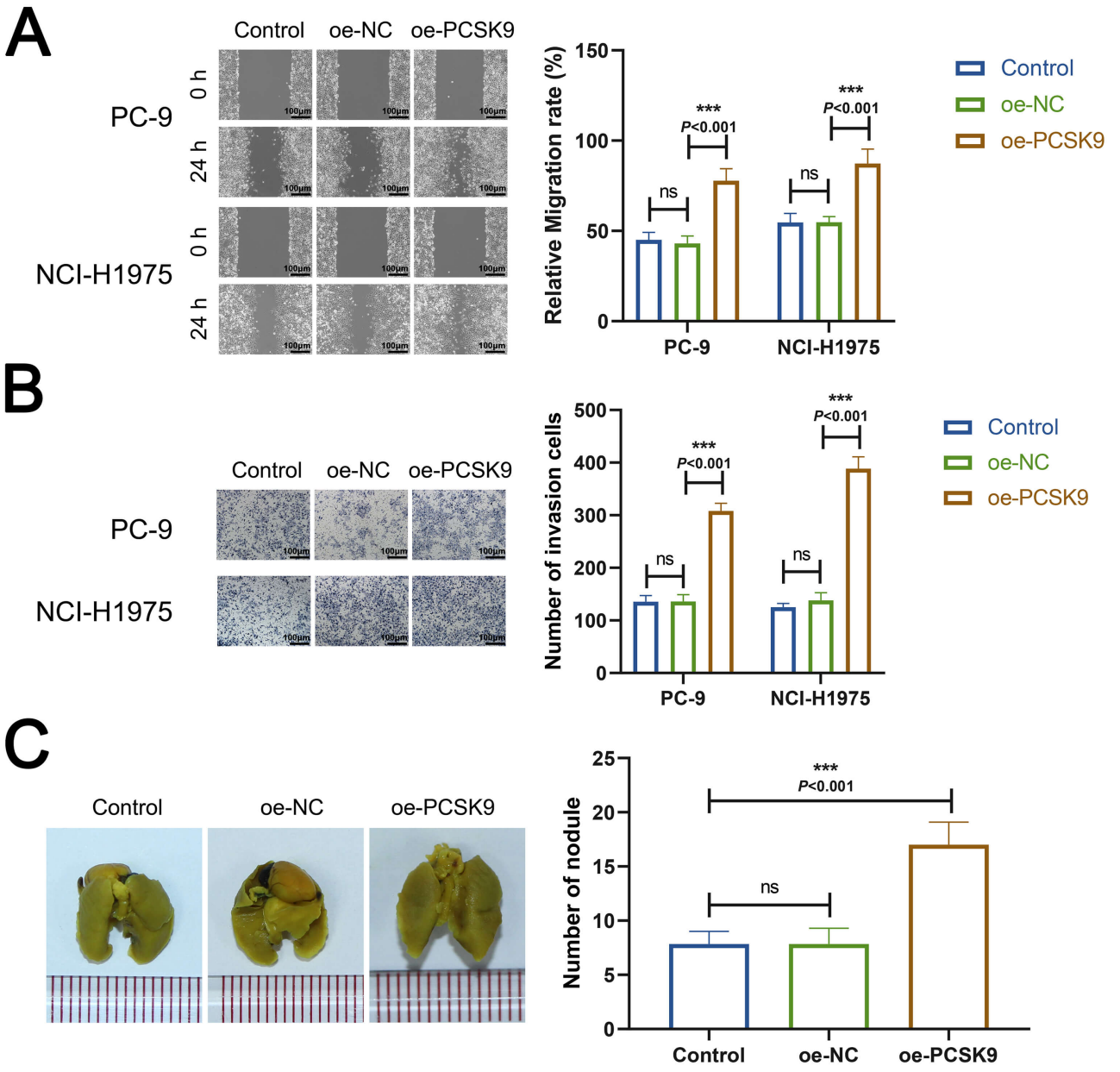

Fig. 4. PCSK9 promotes migration, invasion, and metastasis of LUAD cells. (A) A wound healing assay was conducted to detect the migration ability of cells in the control group and oe-PCSK9 group (Scale bar: 100 μm). n = 3. (B) The Transwell invasion assay was used to verify the effect of PCSK9 on cell invasive ability (Scale bar: 100 μm). n = 3. (C) Lung metastasis status in nude mice following tail vein injection of cells from different treatment groups. n = 6. Data are presented as the mean ± SD. One-way ANOVA was conducted. ns represents no significant, ***$p < 0.001$.

3.2 PCSK9 Promotes the Proliferation of LUAD Cells

In order to elucidate the differential expression of PCSK9, we used Western blotting and qRT-PCR to measure its levels in BEAS-2B and LUAD cell lines. PCSK9 expression was elevated in all LUAD cell lines ($p < 0.001$, Fig. 2A,B). Subsequently, PCSK9 expression was up-regulated in PCSK9 overexpression cell lines, as determined by Western blotting and qPCR ($p < 0.001$, Fig. 2C,D). We subsequently used the CCK-8 assay to examine whether PCSK9 overexpression had an effect on cell proliferation; cell viability was higher in the oe-PCSK9 group ($p < 0.001$, Fig. 2E). Finally, compared to the control group, the apoptotic activity of the oe-PCSK9 group exhibited a downward tendency during TUNEL staining ($p < 0.001$, Fig. 2F).

3.3 PCSK9 Promotes Migration, Invasion and Metastasis of LUAD Cells

We analyzed PCSK9 levels in metastatic and primary LUAD tissues using scRNA-seq data (Fig. 3A). PCSK9

was highly expressed in metastatic LUAD ($p = 0.037$, Fig. 3B). Seven clusters of cell populations were identified (Fig. 3C). To further evaluate how PCSK9 affects LUAD cell migration and invasion, we performed scratch healing and transwell assays. The results demonstrated that in relation to the control and oe-NC groups, the migratory and invasive capacities of LUAD cells influenced by PCSK9 were significantly improved ($p < 0.001$, Fig. 4A). In addition, the oe-PCSK9 group exhibited a significantly enhanced invasive capacity ($p < 0.001$, Fig. 4B). *In vivo* validation confirmed that oe-PCSK9 significantly increased lung metastasis ($p < 0.001$, Fig. 4C), demonstrating that PCSK9 enhances LUAD metastasis.

3.4 The Regulatory Role of PCSK9 in the PI3K/AKT Signaling Pathway

We subsequently performed single-cell pseudotime trajectory analysis of all epithelial cells. The results indicated that normal epithelial cells progressively transitioned into tumor cells over time (Fig. 5A,B). In addition, we identified key genes involved in the cellular transition from epithelial cells to tumor cells, including PCSK9, which was among them (Fig. 5C,D). Next, we identified the functions and pathways associated with these key genes. GO results showed that these genes were enriched in the "generation of precursor metabolites and energy", "focal adhesion", and "antioxidant activity" (Fig. 5E). KEGG results showed that they were involved in "PI3K/AKT signaling" and "chemical carcinogenesis-reactive oxygen species" (Fig. 5F). TCGA-based stratification of patients with LUAD by PCSK9 expression revealed 609 upregulated and 4604 downregulated genes (Fig. 6A). GO and KEGG enrichment analyses were performed to explore the mechanisms of these differentially expressed genes. GO analysis revealed significant enrichment in LUAD-related biological processes, such as "lung development", "collagen-containing extracellular matrix", and "cytokine activity" (Fig. 6B). KEGG analysis indicated a significant accumulation of DEGs within the PI3K/AKT pathway (Fig. 6C).

3.5 PCSK9 Mediates the PI3K/AKT Signaling Pathway to Regulate LUAD Migration, Invasion, and Metastasis

To clarify the regulatory pattern of PCSK9 on the PI3K/AKT pathway, we performed expression profiling of the oe-PCSK9 + MK2206 group and observed that p-AKT, p-PI3K, and p-mTOR levels in the oe-PCSK9 group were markedly elevated (Fig. 7A). In the oe-PCSK9 + MK2206 group, the levels of p-AKT and p-mTOR markedly decreased. Additionally, scratch healing experiments demonstrated that the promoting effect of the oe-PCSK9 group on LUAD was partially reversed by AKT inhibitors (Fig. 7B). Similarly, Transwell invasion experiments also confirmed that the oe-PCSK9 group promoted LUAD through the PI3K/AKT pathway, and MK2206 reduced the promoting effect of PCSK9 on the invasive capacity of LUAD cells (Fig. 7C). Finally, a lung metastasis model was constructed by injecting PC-9 cells into the tail vein, and the results showed that the number of pulmonary metastatic nodules in the oe-PCSK9 group was higher and the infiltration range was wider; the above symptoms were improved in the oe-PCSK9 + MK2206 group (Fig. 7D). The aforementioned cellular experiments and animal models clearly substantiated the pivotal regulatory role of PCSK9.

4. Discussion

The present study confirmed that PCSK9 promotes invasion and metastasis in LUAD, the study was conducted following the research flowchart (Fig. 8). Additionally, we systematically examined the link between PCSK9 expression profiles and the clinical attributes of LUAD, which is essential for guiding therapeutic decisions.

PCSK9 affects the active infiltration of immune cells by downregulating LDLR receptors on their surfaces. When PCSK9 downregulates LDLR on the surface of immune cells, LDL and cholesterol are reduced, and T lymphocytes and natural killer cells cannot obtain sufficient nutrients and enter a dysfunctional state. Once the function of immune cells is impaired, tumor cells are more likely to escape the surveillance of the immune system and gain the opportunity to proliferate and spread [16,17]. Consistent with earlier reports, Kaplan-Meier analysis demonstrated that high PCSK9 expression predicted a poorer prognosis, and PCSK9 mRNA expression was upregulated in LUAD tissues compared to adjacent tissues [18,19]. The ROC curve further indicated that PCSK9 exhibited a good diagnostic efficacy for LUAD.

To further investigate the molecular mechanism of PCSK9, we performed cellular experiments. PCSK9 expression was elevated in all LUAD cell lines, and elevated expression of PCSK9 promoted cell migration and invasion. In addition, scRNA-seq data showed that PCSK9 is highly expressed in metastatic LUAD. Similarly, *in vivo* mouse lung metastasis models have further confirmed this hypothesis. Both the scRNA-seq and TCGA datasets demonstrated that the PI3K/AKT pathway is critically involved in LUAD tumorigenesis. PI3K/AKT, a signal transduction pathway regulating cell growth and proliferation, can accelerate invasive and metastatic activities through multiple mechanisms, as supported by several studies [20,21]. Specifically, PI3K is activated when upstream signaling molecules and cell membrane surface receptors specifically bind, which enables the conversion of PIP3, and the activation of PI3K is mediated by the interaction of upstream signaling molecules and cell membrane surface receptors, after conversion, PIP3 can recruit and phosphorylate AKT (protein kinase B) to the cell membrane, forming an active phosphorylated AKT (p-AKT), which ultimately drives the migration and invasion process of LUAD cells [22]. Western blotting further confirmed that PCSK9

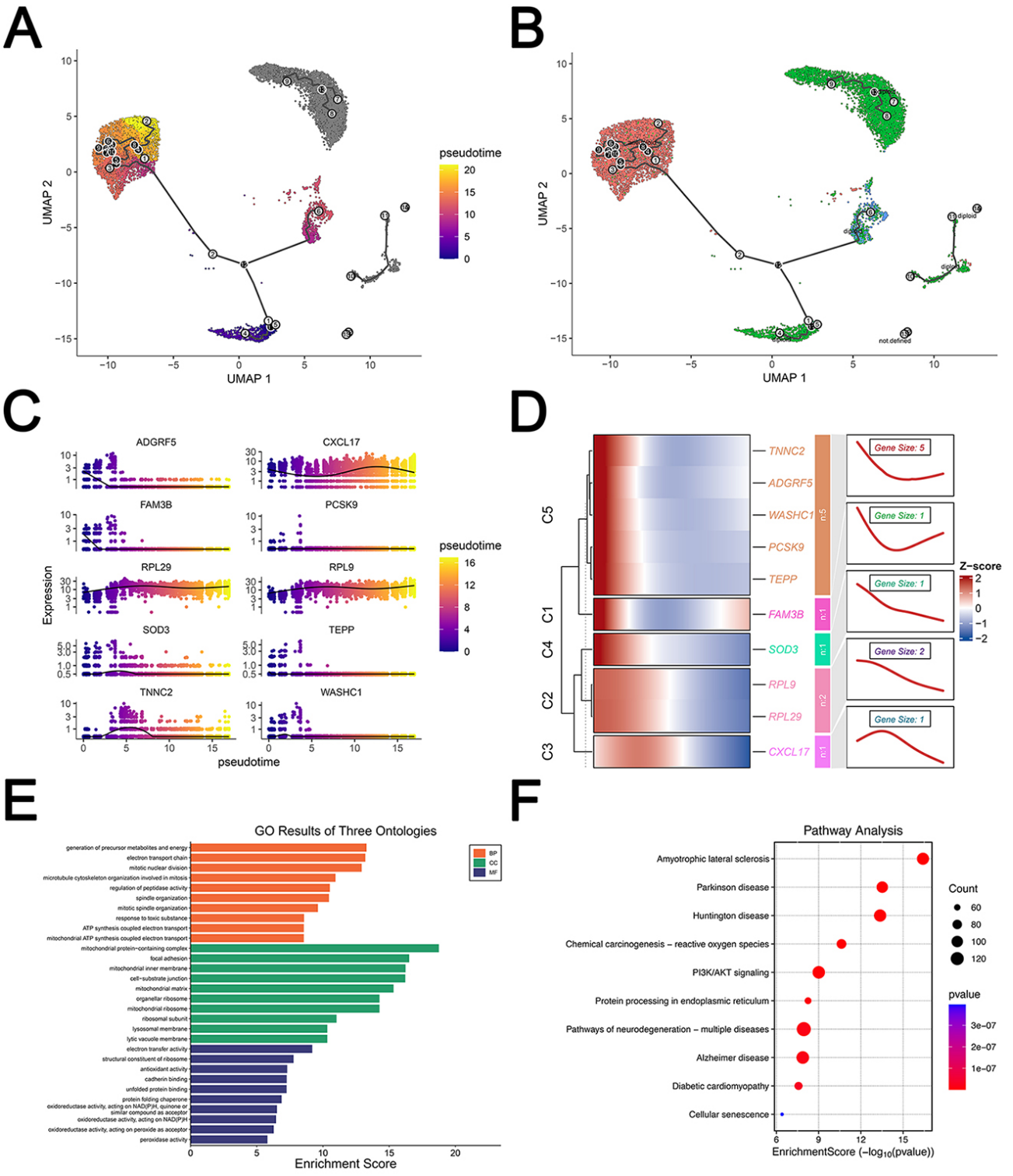

Fig. 5. Pseudotime trajectory analysis and enrichment analysis. (A) Pseudotime trajectory analysis of epithelial cells. (B) Pseudotime trajectory analysis of the transition from epithelial cells to tumor cells. Red: tumor cells; green: epithelial cells. (C) Identifying genes that change as a function of pseudotime. (D) The expression of pseudotime-related genes in epithelial cells and tumor cells. (E,F) GO and KEGG pathway enrichment analysis of pseudotime-related genes. GO, Gene Ontology; KEGG, Kyoto Encyclopedia of Genes and Genomes.

overexpression significantly increased the p-AKT levels. To test this hypothesis, we treated LUAD cells overexpressing an AKT inhibitor (MK2206) and found that MK2206 reversed the invasive effects of PCSK9 on LUAD cells. Con-

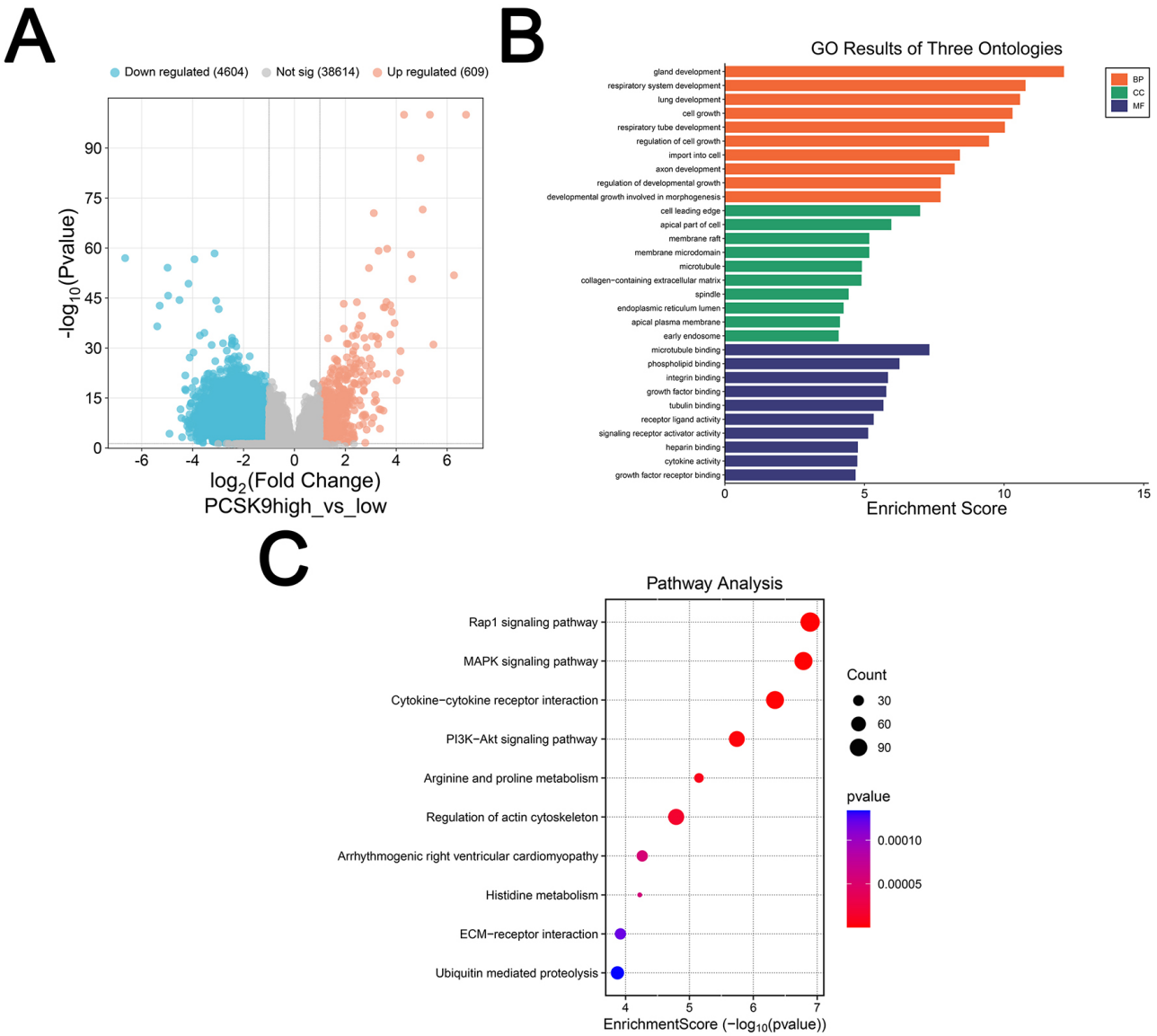

Fig. 6. PCSK9 activates the PI3K/AKT pathway. (A) Volcano plot showing DEGs between the high- and low-PCSK9 expression groups. (B,C) GO and KEGG pathway enrichment analysis of DEGs. PI3K/AKT, phosphoinositide 3-kinase/protein kinase B.

sistent results were obtained in an *in vivo* mouse lung metastasis model. It has been shown that the PI3K/AKT pathway is a key driver of LUAD tumor development.

Our findings extend our current understanding of PCSK9 in LUAD in several ways. Our study is the first to demonstrate, using scRNA-seq analysis, that PCSK9 is specifically enriched in malignant epithelial cells and is associated with EMT at single-cell resolution. Moreover, we provide the first causal evidence through pharmacological rescue experiments that AKT inhibition partially reverses PCSK9-driven proliferation, migration, and invasion, as well as *in vivo* lung metastasis. This level of mechanistic validation positions our study as a significant advancement in the understanding of PCSK9's role in LUAD progression.

5. Limitations

However, this study had certain limitations. First, the small sample size undermined the accuracy and reliability of the findings. The diagnostic and prognostic value of PCSK9 needs to be validated in larger multicenter prospective cohorts to enhance the generalizability of our findings. Another limitation of the current study is the lack of functional loss experiments. While our overexpression data, clinical correlation, and rescue experiments provide strong evidence for the oncogenic role of PCSK9 in LUAD, future studies employing genetic silencing approaches will be valuable to further validate these findings and explore the therapeutic potential of PCSK9 inhibition. Additionally, the upstream mechanism of PCSK9 activation and the downstream effect of the PI3K/AKT pathway remain unclear. Further studies, including co-immunoprecipitation

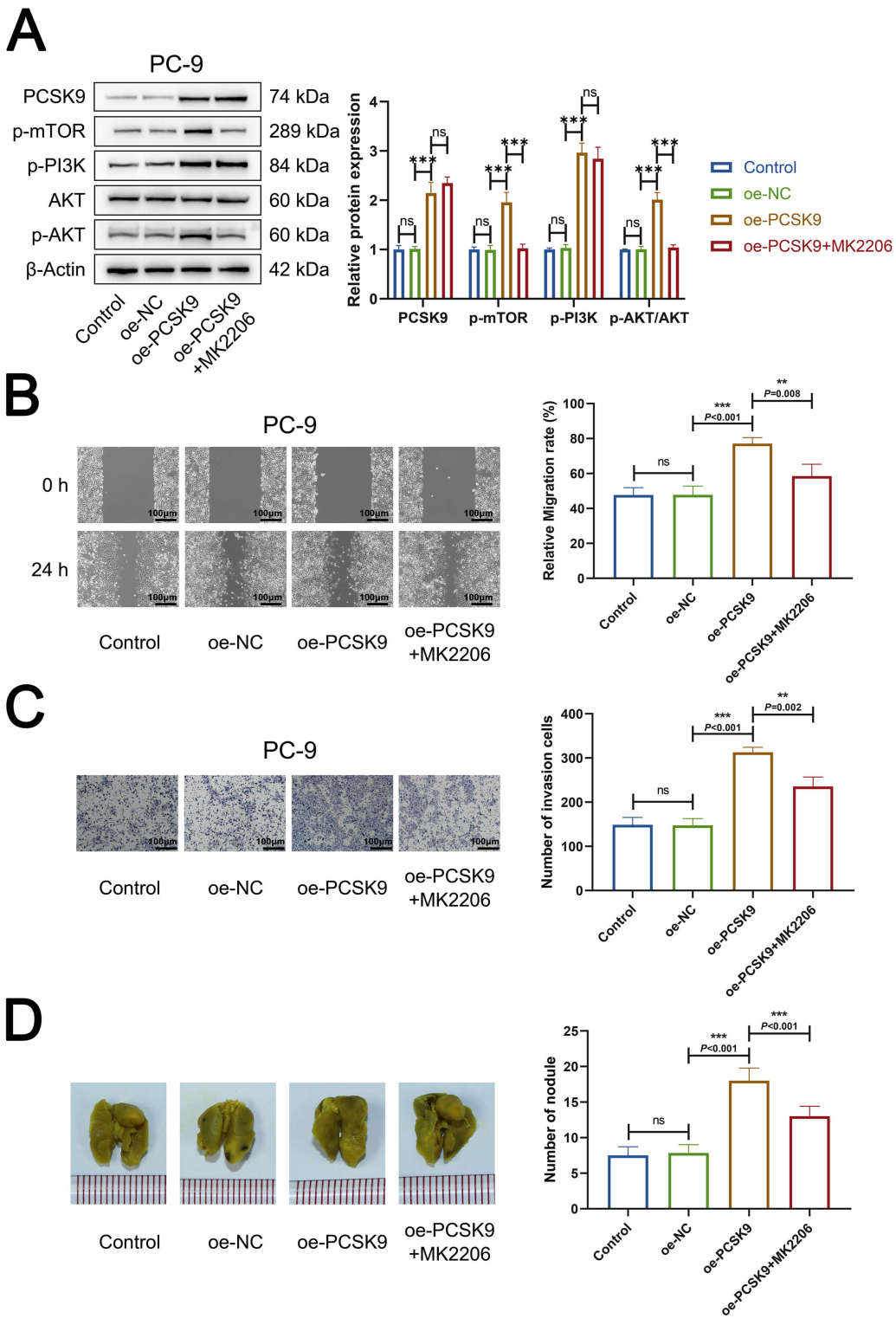

Fig. 7. PCSK9 regulates the migration, invasion, and metastasis of LUAD via the PI3K/AKT pathway. (A) Western blotting results showed the levels of PCSK9, p-PI3K, p-AKT, AKT, and p-mTOR. n = 3. (B) Wound healing assay for detecting the migration ability of LUAD cells in different treatment groups (Scale bar: 100 μm). n = 3. (C) Transwell invasion assay was performed to verify the effect of MK2206 on the invasive ability of LUAD cells (Scale bar: 100 μm). n = 3. (D) The status of lung metastasis in mice following tail vein injection. n = 6. Data are presented as the mean ± SD. One-way ANOVA was conducted. ns represents no significant, $^{**}p < 0.01$, $^{***}p < 0.001$. p-PI3K, phosphorylated phosphatidylinositol 3-kinase; p-AKT, phosphorylated protein kinase B; p-mTOR, phosphorylated mammalian target of rapamycin.

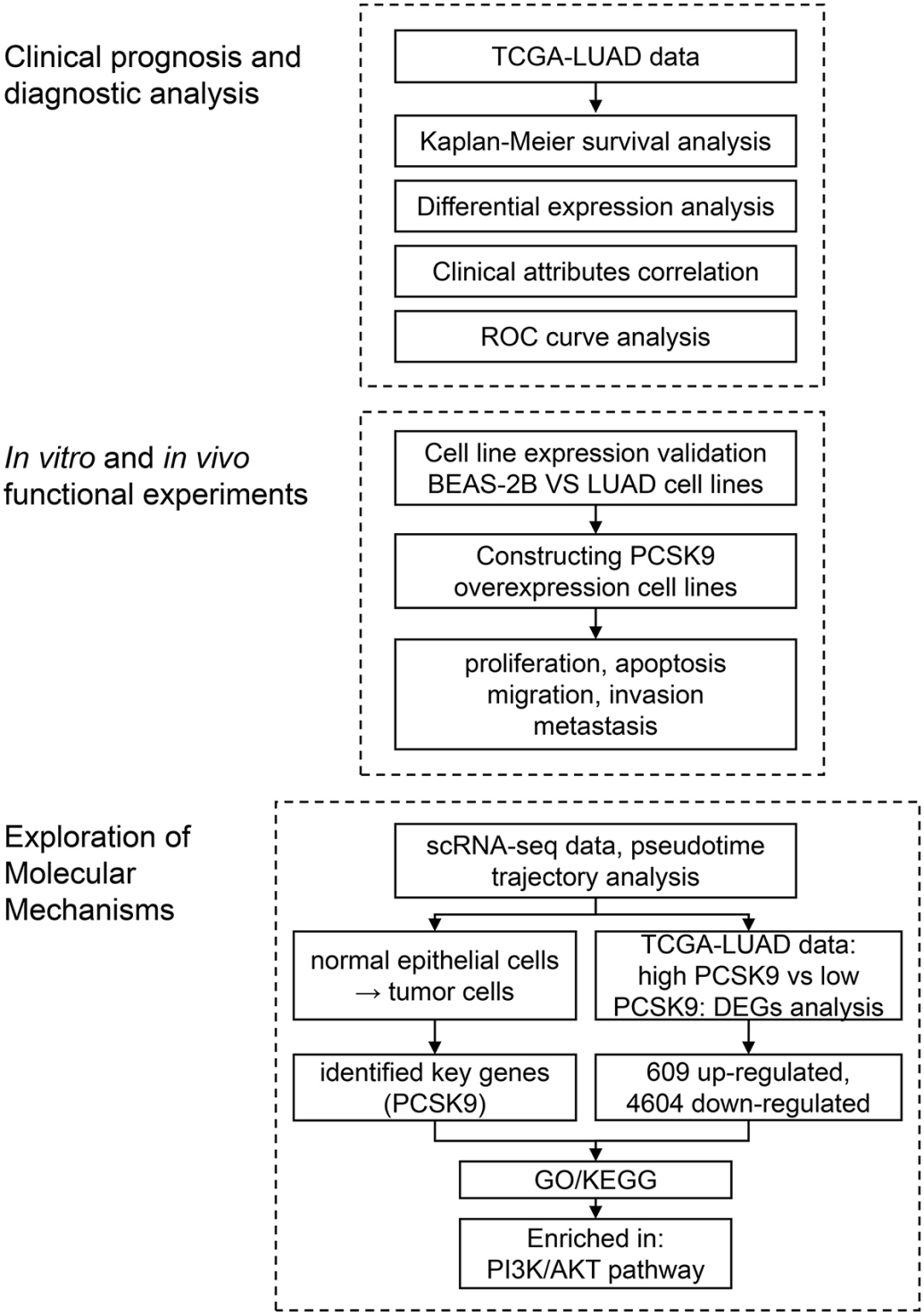

Fig. 8. Schematic diagram illustrating the comprehensive study design, bioinformatic analysis, and experimental validation workflow. TCGA, The Cancer Genome Atlas Program; scRNA-seq, single-cell RNA sequencing.

and mutagenesis assays, are required to identify the direct binding partners of PCSK9 in LUAD. Fourth, regarding the mouse model, although quantification of lung metastasis by counting surface nodules is widely used and accepted in experimental metastasis studies, future investigations employing serial sectioning and immunohistochemical analysis of whole lungs would provide a more comprehensive assessment of metastatic dissemination. Direct validation of PCSK9 expression and PI3K/AKT pathway activation in metastatic lesions in a mouse model would provide stronger *in vivo* evidence for the proposed mechanism. More importantly, the *in vivo* lung metastasis model utilized (tail vein

injection) primarily reflects the later stages of metastatic colonization, rather than the entire process of local invasion and intravasation. Future studies employing orthotopic implantation models should provide a more comprehensive assessment of PCSK9's role in the metastatic cascade. Finally, the cross-regulation and synergistic effects between PCSK9 and other key signaling pathways (such as MAPK) have not been verified by functional experiments, such as dual-luciferase reporter gene assay and Co-IP, which results in a one-sided understanding of its functional network in the development of LUAD. In the future, we can compensate for these shortcomings and conduct an in-depth exploration.

6. Conclusions

In summary, PCSK9 promoted the invasion and metastasis of LUAD cells via activation of the PI3K/AKT pathway. Furthermore, its association with LUAD prognosis and diagnosis offers a theoretical basis for its potential clinical applications.

Abbreviations

LUAD, lung adenocarcinoma; PCSK9, proprotein convertase subtilisin/kexin type 9; IARC, International Agency for Research on Cancer; LDL, low-density lipoprotein; LDLR, low-density lipoprotein receptors; PI3K/AKT, phosphoinositide 3-kinase/protein kinase B; TCGA, The Cancer Genome Atlas; FC, fold change; GO, Gene Ontology; KEGG, Kyoto Encyclopedia of Genes and Genomes; qRT-PCR, Quantitative reverse transcription polymerase chain reaction; ATCC, American Type Culture Collection; FBS, Fetal Bovine Serum; NCBI, National Center for Biotechnology Information; SDS-PAGE, Sodium Dodecyl Sulfate-Polyacrylamide Gel Electrophoresis; PVDF, Polyvinylidene Fluoride; TBST, Tween-20-supplemented Tris-buffered saline; p-AKT, phosphorylated AKT; CCK-8, Cell Counting Kit-8; OD, Optical Density; scRNA-seq, single-cell RNA sequencing; GEO, Gene Expression Omnibus; PCA, principal component analysis; UMAP, uniform manifold approximation and projection; PBS, phosphate-buffered saline; SPF, Specific Pathogen Free; SD, standard deviation; ROC, Receiver operating characteristic; AUC, area under the curve; OS, overall survival; DFS, disease-free survival.

Availability of Data and Materials

The original data presented in this study are included in the article and Supplementary Material. Further inquiries can be directed to the corresponding authors.

Author Contributions

Conceptualization, DZ and DJW; Methodology, LXQ and NJ; Validation, LJZ and CC; Formal Analysis, XH and DZ; Investigation, DJW; Resources, XH; Data Curation, LXQ and NJ; Writing —Original Draft Preparation, DZ and DJW; Writing — Review & Editing, CC and XH; Visualization, NJ and LJZ; Supervision, LXQ; Project Administration, XH; Funding Acquisition, XH. All authors contributed to editorial changes in the manuscript. All authors read and approved the final manuscript. All authors have participated sufficiently in the work and agreed to be accountable for all aspects of the work.

Ethics Approval and Consent to Participate

The study involving human participants was conducted in accordance with the Declaration of Helsinki. The research protocol was approved by the Ethics Committee of Jiangsu Cancer Hospital (Ethic Approval Number: 2021-017). Written informed consent was obtained from 100 patients prior to the study for the use of biological samples in the experiments and data analysis. The study involving animal experiments was approved by Jiangsu Cancer Hospital Institutional Animal Care and Use Committee (No. IACUC-001-31). The study was carried out in accordance with the ARRIVE guidelines and complied with the NIH Guide for the Care and Use of Laboratory Animals.

Acknowledgment

We gratefully acknowledge the assistance and instruction from all investigators who participated.

Funding

This research was funded by the Science and Technology Development Fund of Jiangsu Cancer Hospital (XHMS202408 and XHQN202409).

Conflicts of Interest

The authors declare no conflicts of interest.

Supplementary Material

Supplementary material associated with this article can be found in the online version, at https://doi.org/10.31083/FBL49685.

References

[1] Bade BC, Dela Cruz CS. Lung Cancer 2020: Epidemiology, Etiology, and Prevention. Clinics in Chest Medicine. 2020; 41: 1–24. https://doi.org/10.1016/j.ccm.2019.10.001

[2] Dela Cruz CS, Tanoue LT, Matthay RA. Lung cancer: epidemiology, etiology, and prevention. Clinics in Chest Medicine. 2011; 32: 605–644. https://doi.org/10.1016/j.ccm.2011.09.001

[3] Schabath MB, Cote ML. Cancer Progress and Priorities: Lung Cancer. Cancer Epidemiology, Biomarkers & Prevention : a Publication of the American Association for Cancer Research, Cosponsored by the American Society of Preventive Oncology. 2019; 28: 1563–1579. https://doi.org/10.1158/1055-9965.EPI-19-0221

[4] Chen Y, Xiang T. SGO2 as a Prognostic Biomarker Correlated with Cell Proliferation, Migration, Invasion, and Epithelial-Mesenchymal Transition in Lung Adenocarcinoma.Frontiers in Bioscience (Landmark edition).2024; 29: 314. https://doi.org/10.31083/j.fbl2909314

[5] Wei X, Li X, Hu S, Cheng J, Cai R. Regulation of Ferroptosis in Lung Adenocarcinoma. International Journal of Molecular Sciences. 2023; 24: 14614. https://doi.org/10.3390/ijms241914614
[6] Chen JW, Dhahbi J. Lung adenocarcinoma and lung squamous cell carcinoma cancer classification, biomarker identification, and gene expression analysis using overlapping feature selection methods. Scientific Reports. 2021; 11: 13323. https://doi.org/10.1038/s41598-021-92725-8
[7] Roth EM, Davidson MH. PCSK9 Inhibitors: Mechanism of Action, Efficacy, and Safety. Reviews in Cardiovascular Medicine. 2018; 19: S31–S46. https://doi.org/10.3909/ricm19S1S0002
[8] Melendez QM, Krishnaji ST, Wooten CJ, Lopez D. Hypercholesterolemia: The role of PCSK9. Archives of Biochemistry and Biophysics. 2017; 625-626: 39–53. https://doi.org/10.1016/j.abb.2017.06.001
[9] Sotler T, Šebeštjen M. PCSK9 as an Atherothrombotic Risk Factor. International Journal of Molecular Sciences. 2023; 24: 1966. https://doi.org/10.3390/ijms24031966
[10] Wang L, Li S, Luo H, Lu Q, Yu S. PCSK9 promotes the progression and metastasis of colon cancer cells through regulation of EMT and PI3K/AKT signaling in tumor cells and phenotypic polarization of macrophages. Journal of Experimental & Clinical Cancer Research : CR. 2022; 41: 303. https://doi.org/10.1186/s13046-022-02477-0
[11] Wong CC, Wu JL, Ji F, Kang W, Bian X, Chen H, et al. The cholesterol uptake regulator PCSK9 promotes and is a therapeutic target in APC/KRAS-mutant colorectal cancer. Nature Communications. 2022; 13: 3971. https://doi.org/10.1038/s41467-022-31663-z
[12] Bonaventura A, Grossi F, Montecucco F. PCSK9 is a promising prognostic marker in patients with advanced NSCLC. Cancer Immunology, Immunotherapy : CII. 2020; 69: 491–492. https://doi.org/10.1007/s00262-020-02485-z
[13] Bai H, Li Z, Weng Y, Cui F, Chen W. Integrated analysis of single-cell RNA-seq and bulk RNA-seq revealed key genes for bone metastasis and chemoresistance in prostate cancer. Genes & Genomics. 2024; 46: 1445–1460. https://doi.org/10.1007/s13258-024-01575-x
[14] Zhao S, Zhang P, Niu S, Xie J, Liu Y, Liu Y, et al. Targeting nucleotide metabolic pathways in colorectal cancer by integrating scRNA-seq, spatial transcriptome, and bulk RNA-seq data. Functional & Integrative Genomics. 2024; 24: 72. https://doi.org/10.1007/s10142-024-01356-5
[15] Yu G, Wang LG, Han Y, He QY. clusterProfiler: an R package for comparing biological themes among gene clusters. Omics : a Journal of Integrative Biology. 2012; 16: 284–287. https://doi.org/10.1089/omi.2011.0118
[16] Nicholls SJ. PCSK9 inhibitors and reduction in cardiovascular events: Current evidence and future perspectives. Kardiologia Polska. 2023; 81: 115–122. https://doi.org/10.33963/KP.a2023.0030
[17] Bao X, Liang Y, Chang H, Cai T, Feng B, Gordon K, et al. Targeting proprotein convertase subtilisin/kexin type 9 (PCSK9): from bench to bedside. Signal Transduction and Targeted Therapy. 2024; 9: 13. https://doi.org/10.1038/s41392-023-01690-3
[18] Oza PP, Kashfi K. The evolving landscape of PCSK9 inhibition in cancer. European Journal of Pharmacology. 2023; 949: 175721. https://doi.org/10.1016/j.ejphar.2023.175721
[19] Quagliariello V, Bisceglia I, Berretta M, Iovine M, Canale ML, Maurea C, et al. PCSK9 Inhibitors in Cancer Patients Treated with Immune-Checkpoint Inhibitors to Reduce Cardiovascular Events: New Frontiers in Cardioncology. Cancers. 2023; 15: 1397. https://doi.org/10.3390/cancers15051397
[20] Wei C, Dong X, Lu H, Tong F, Chen L, Zhang R, et al. LPCAT1 promotes brain metastasis of lung adenocarcinoma by up-regulating PI3K/AKT/MYC pathway. Journal of Experimental & Clinical Cancer Research : CR. 2019; 38: 95. https://doi.org/10.1186/s13046-019-1092-4
[21] Li Z, Zhao PL, Gao X, Li X, Meng YQ, Li ZQ, et al. DUS4L suppresses invasion and metastasis in LUAD via modulation of PI3K/AKT and ERK/MAPK signaling through GRB2. International Immunopharmacology. 2024; 142: 113043. https://doi.org/10.1016/j.intimp.2024.113043
[22] Noorolyai S, Shajari N, Baghbani E, Sadreddini S, Baradaran B. The relation between PI3K/AKT signalling pathway and cancer. Gene. 2019; 698: 120–128. https://doi.org/10.1016/j.gene.2019.02.076